

# Lattice Study of QCD Phase Structure by Canonical Approach

D. Boyda<sup>a,b,c,\*</sup>, V.G. Bornyakov<sup>f,b</sup>, V. Goy<sup>b,c</sup>, A. Molochkov<sup>b</sup>,  
A. Nakamura<sup>b,d,e</sup>, A. Nikolaev<sup>b</sup>, V.I. Zakharov<sup>b,c,g</sup>

<sup>a</sup> *School of Natural Sciences, Far Eastern Federal University (FEFU),  
Sukhanova 8, Vladivostok 690950, Russia*

<sup>b</sup> *School of Biomedicine, Far Eastern Federal University (FEFU),  
Sukhanova 8, Vladivostok 690950, Russia*

<sup>c</sup> *Institute of Theoretical and Experimental Physics NRC Kurchatov Institute, 117218  
Moscow, Russia*

<sup>d</sup> *Theoretical Research Division, Nishina Center, RIKEN, Wako 351-0198, Japan*

<sup>e</sup> *Research Center for Nuclear Physics (RCNP), Osaka University, Ibaraki, Osaka,  
567-0047, Japan*

<sup>f</sup> *Institute for High Energy Physics NRC Kurchatov Institute, 142281 Protvino, Russia*

<sup>g</sup> *Moscow Institute of Physics and Technology, Dolgoprudny, Moscow Region, 141700  
Russia*

---

## Abstract

We investigate the potential for using the canonical ensemble approach to determine the QCD phase diagram in the temperature - density plane. This approach allows us to study the finite baryon density regions where the well-known sign problem obstructs the standard lattice QCD numerical study. In the canonical ensemble approach, we perform lattice QCD simulations at the pure imaginary quark chemical potential. In this case no sign problem occurs. We then calculate physical quantities at the real chemical potential through the canonical partition functions.

In this approach, the canonical partition functions,  $Z_n$ , play an essential role for mapping the information from the pure imaginary chemical potential values to the real ones. We analyze how inaccuracies in the numerical data obtained at the imaginary chemical potential affect the results for the real values, where the QCD predictions confront experimental quark-gluon plasma data.

---

\*Corresponding author (boyda\_d@mail.ru)

We compute the higher moments of the baryon number density including the kurtosis, and compare our results with information from relativistic heavy-ion collision experiments.

*Keywords:* lattice QCD, quark gluon plasma, QCD phase diagram, finite density, sign problem, canonical partition function

*PACS:* , 12.38.Mh, 21.65.Qr, 24.85.+p, 25.75.-q

---

## 1. Introduction

Many studies have tried to reveal the properties of strongly interacting quark-gluon/hadron matter from experimental and phenomenological analyses of high-energy heavy-ion collisions [1, 2, 3, 4]. It is expected that these studies will lead to understanding of the phase diagram in the temperature - baryon density plane, which is also looked for in cosmological research. The first principle calculations, based on lattice QCD, have a potential to provide reliable fundamental information in this active area of research. However, to obtain this information, we must first overcome the “sign problem”, which is described below.

The lattice QCD is a simulation study based on the grand canonical partition function,

$$Z_{GC}(\mu, T, V) = \int \mathcal{D}U (\det \Delta(\mu))^{N_f} e^{-S_G}. \quad (1)$$

Here  $\det \Delta$  is the fermion determinant satisfying the relation

$$[\det \Delta(\mu)]^* = \det \Delta(-\mu^*). \quad (2)$$

Consequently, when  $\mu$  is real,  $\det \Delta$  is complex, and when  $\mu$  is pure imaginary,  $\det \Delta$  is real.

In Monte Carlo simulations, the gluon fields,  $U$ , are generated with the probability proportional to the integrand in Eq. (1), and therefore, if  $\det \Delta$  is complex, the simulations cannot be conducted. If we separate out the phase factor, i.e. rewrite the integrand as

$$(|(\det \Delta)|e^{i\theta})^{N_f} e^{-S_G} \quad (3)$$

and include only the absolute value into the probability then the observables include the phase and oscillate. This makes the simulation practically impossible, and is called the “sign problem”.

In order to circumvent this obstacle, many approaches have been pursued, see [5] for recent review. In recent publications [6, 7, 8, 9] where higher order cumulants were evaluated for nearly physical quark masses, mostly Taylor expansion method was employed and simulations were performed at zero chemical potential. Monte Carlo simulations for pure imaginary  $\mu$  are free from the complex measure problem, as can be seen from Eq. (2). The question is how can one extract data for real  $\mu$ ?

The grand canonical partition function is related to the canonical partition function,  $Z_C(n, T, V)$ , as follows:

$$\begin{aligned} Z_{GC}(\mu, T, V) &= \text{Tr} (e^{-\frac{\hat{H} - \mu \hat{N}}{T}}) = \sum_{n=-\infty}^{\infty} \langle n | e^{-\frac{\hat{H}}{T}} | n \rangle e^{\frac{\mu n}{T}} \\ &= \sum_{n=-\infty}^{\infty} Z_C(n, T, V) e^{\frac{\mu n}{T}} = \sum_{n=-\infty}^{\infty} Z_n \xi^n, \end{aligned} \quad (4)$$

where  $\xi = e^{\mu/T}$  is the fugacity,  $\hat{N}$  is an operator of a conserved quantum number such as a baryon number or electric charge and we introduced abbreviation  $Z_n$  for  $Z_C(n, T, V)$ . In this letter, we are mainly concerned with the baryon number case.

For imaginary  $\mu$  ( $\mu = i\mu_I$  and  $\theta_I = \mu_I/T$ ), we can calculate  $Z_n$  by the inverse Fourier transformation [10] as

$$Z_n = \int_0^{2\pi} \frac{d\theta_I}{2\pi} e^{-in\theta_I} Z_{GC}(\mu = i\theta_I T, T, V). \quad (5)$$

Note that  $Z_n = \langle n | e^{-\frac{\hat{H}}{T}} | n \rangle$  does not depend on  $\mu$ , and therefore one can evaluate the grand canonical partition function,  $Z_{GC}$ , in Eq.(4) for any  $\mu$  (imaginary or real) once  $Z_n$  are known.

Now we have a route from the imaginary to the real chemical potential regions:

- Step 1: Using Eq. (5), we calculate  $Z_n$  from  $Z_{GC}$  computed at the imaginary  $\mu$ .
- Step 2: Substituting these  $Z_n$  into Eq. (4), we construct  $Z_{GC}$  for the real  $\mu$ .

When searching for the phase transition, the following moments,  $\lambda_m$ , are often employed in heavy ion collision experiments:

$$\lambda_m(\mu) = \left(T \frac{\partial}{\partial \mu}\right)^m \log Z_{GC} = \left(\xi \frac{\partial}{\partial \xi}\right)^m \log \left(\sum_{n=-\infty}^{\infty} Z_n \xi^n\right). \quad (6)$$

Especially,  $\lambda_2$  (susceptibility),  $\lambda_3$ , and  $\lambda_4$ , provide useful information on the phase structure. In this paper we investigate the potential of the canonical ensemble approach to reveal the QCD phases.

## 2. Lattice Setup

In order to simulate the lattice QCD at the imaginary quark chemical potential we employ the clover improved Wilson fermion action. The chemical potential  $\mu$  couples with the fourth component of the current  $\bar{\psi}\gamma_4\psi$  in the Euclidean path-integral, then a temporal hop accompanies a factor  $e^{\pm\mu a}$ . For the gauge field action,  $S_G$ , we use the Iwasaki gauge action. The lattice size is  $4 \times 16^3$ .

The values of parameters of the fermion matrix  $\Delta$ , i.e. the hopping parameter  $\kappa$  and the coefficient of the clover term,  $C_{SW}$  were taken from Ref. [11]. Our simulation corresponds to  $m_\pi/m_\rho = 0.8$  ( $m_\pi = 0.7$  GeV). We study two temperatures:  $T/T_c = 1.35(7)$  ( $\beta = 2.0$ ) corresponds to the deconfinement phase and  $T_c = 0.93(5)$  ( $\beta = 1.8$ ) - the confinement phase.

In the confinement (deconfinement) phase we make simulations at 27(37) different values of the baryon chemical potential  $\mu_I$  in the interval  $0 \leq \mu_I/T \leq \pi$ . Additionally we make simulations at a few values of  $\mu_I$  above  $\pi$  to check the Roberge-Weiss periodicity. For each value of  $\mu_I$  1800 configurations separated by ten trajectories are used to evaluate the physical observables.

## 3. Determination of $Z_n$

We can evaluate the baryon number density  $n_B$  directly, for any value of the imaginary chemical potential, using standard lattice QCD algorithms:

$$\frac{n_B}{T^3} = i \frac{N_f N_t^3}{N_s^3 Z_{GC}} \int \mathcal{D}U e^{-S_G} (\det \Delta(\mu_I))^{N_f} \text{Tr} \left[ \Delta^{-1} \frac{\partial \Delta}{\partial \mu_I/T} \right]. \quad (7)$$

On the other hand, the number density is connected with the canonical partition function,  $Z_n$  as

$$n_B = \frac{\lambda_1}{V} = \frac{T}{V} \frac{\partial}{\partial \mu} \ln Z_{GC}(\mu, T) = \frac{i}{(aN_s)^3} \frac{2 \sum_{n=1}^{\infty} Z_n n \sin(n\theta_I)}{Z_0 + 2 \sum_{n=1}^{\infty} Z_n \cos(n\theta_I)}, \quad (8)$$

where we used Eq. (4) and relation  $Z_n = Z_{-n}$ . The direct way to extract the canonical partition functions  $Z_n$  from the lattice data for  $n_B$  is to fit it to Eq. (8) with  $Z_n$  as fitting parameters. We tried to do it and realized that the fit goes quite unstable and some  $Z_n$ 's are negative. The difficulty of fitting comes from the drastic cancellations in both the numerator and denominator in Eq.(8).

More promising way is to construct the grand canonical partition function from  $n_B$ . Integrating Eq. (8) over imaginary  $\mu_I$ , at fixed temperature  $T$ , we have

$$\frac{Z_{GC}(\theta_I)}{Z_{GC}(0)} = \exp \left( V \int_0^{\theta_I} d(i\tilde{\theta}_I) i \operatorname{Im}[n_B(\tilde{\theta}_I)] \right) = \exp \left( -V \int_0^{\theta_I} dx n_{BI}(x) \right), \quad (9)$$

where we use the fact that  $n_B$  is pure imaginary and denote  $n_{BI} = \operatorname{Im} n_B$ . We calculate  $Z_n$  by inserting this  $Z_{GC}$  into Eq (5). Then one can construct  $Z_{GC}$  as  $Z_{GC} = \sum Z_n \xi^n$  at real  $\mu$ . This procedure provides a new method to study physics in the real chemical potential region via Monte Carlo simulations of the pure imaginary chemical potential [12, 13].

There is no Ansatz until this point; therefore, Eq. (9) is exact and theoretically the calculation for any value of the chemical potential is possible. In practice, however, we must introduce some assumptions, and consequently, the reliable range of the real chemical potential values is restricted.

One way to evaluate the right hand side in Eq. (9) is to calculate the number density for many values of  $\mu_I$  and complete the numerical integration. In order to obtain a reliable result, we need hundreds of different  $\mu_I$  values, but this is computationally expensive task. In this letter we employ a simple approach - instead of using  $n_B$ , calculated directly with lattice QCD, we parametrize it with some function.

The idea to fit physical quantities as a function of  $\mu_I$  and to extrapolate to the real  $\mu$  comes back to Refs. [14] and [15]. The authors of Ref. [8] have recently reported a thorough analysis. In Refs. [16], the authors pointed out that the number density for the imaginary chemical potential is well

approximated by a Fourier series at  $T < T_c$ ,

$$n_{BI}(\theta_I)/T^3 = \sum_{k=1}^{\infty} f_{3k} \sin(k\theta_I), \quad (10)$$

and by a polynomial series at  $T > T_c$ ,

$$n_{BI}(\theta_I)/T^3 = \sum_{k=1}^{\infty} a_{2k-1} \theta_I^{2k-1}. \quad (11)$$

In Refs. [12, 13] we confirmed these conclusions with higher precision. Therefore in the present study in computation of  $Z_{GC}(\theta)/Z_{GC}(0)$  we use parametrizations Eqs. (10) and (11). We obtained  $f_3 = 0.0871(3)$ ,  $f_6 = -0.00032(27)$  ( $\chi^2/dof = 0.93$ ) and  $a_1 = 1.5570(7)$ ,  $a_3 = -0.3300(13)$  ( $\chi^2/dof = 0.67$ ) for our data  $n_{BI}$ .

Actually this assumption may result in a systematic error due to cutting number of terms in Eqs. (10) and (11), where each coefficient has the statistical errors. To estimate this statistical error in detail, we apply a version of a bootstrap method: Here one bootstrap sample consists of a set of standard bootstrap samples of the number density created for every value of  $\mu_I$ . On each bootstrap sample we estimate  $n_B$  with Eq. (10) ( $T < T_c$ ) or Eq. (11) ( $T > T_c$ ) (coefficients  $f_{3k}$  or  $a_{2k-1}$  are different on each sample), and calculate  $Z_n$  according to Eqs. (9) and (5). Then, using these  $Z_n$  and Eq. (6) with number of terms restricted to  $n_{max}$ , we calculate observables.

In Refs. [12, 16], the baryon number density fitted to Eqs. (10) or (11) was analytically continued to the real chemical potential values. This method has a drawback. First, the phase transition location may be missed because of the breaking of analyticity. Second, it is difficult how to determine the reliable range of this analytic continuation. Canonical approach provides us information on the reliable range from the fact that  $Z_n$  must be positive. We check that  $Z_n$  should be positive for all  $n \leq n_{max}$  in all bootstrap samples used in the statistical analysis as described above. We then compute observables from Eq. (6) using  $Z_n$  for  $n \leq n_{max}$ . Respective result for the number density coincides with that obtained via analytic continuation at small enough values of  $\mu/T$ . However, it starts to deviate at larger values of  $\mu/T$ . The value of  $\mu/T$  where this deviation becomes substantial determines the range of reliability of the analytic continuation. We will illustrate this procedure in the next section.

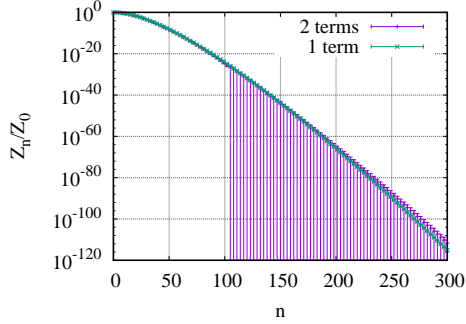


Figure 1: Normalized  $Z_n$  as a function of  $n$  obtained by the integration method.  $T/T_c = 0.93$  (Confinement).

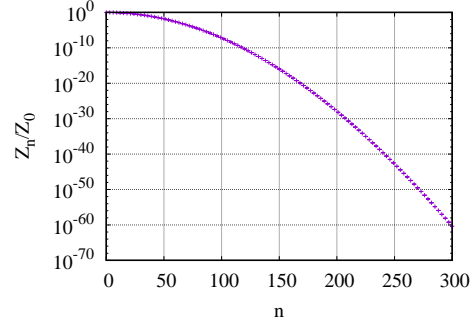


Figure 2: Normalized  $Z_n$  as a function of  $n$  obtained by the integration method.  $T/T_c = 1.35$  (Deconfinement). HPE stands for the hopping parameter expansion.

In the Fig. 1 one can see  $Z_n/Z_0$  calculated with one term and two terms in Eq. (10). The error of two-term ansatz is large due to propagation of large relative error of  $f_6$ , i.e. noise from our statistics. There is also a discrepancy between two results although it is insignificant within error bars.

We have compared our results for  $Z_n$  with winding number expansion method and found good agreement. Also we extracted Taylor coefficients from our observables and compared it with the Taylor expansion approach. For details, see Ref. [12].

#### 4. Physical quantities

It is now straightforward to calculate the number density, the pressure and the baryon number moments.

##### Baryon number density

Using our  $Z_n$  that were calculated with two terms Fourier ansatz in the confinement phase and two terms polynomial ansatz in the deconfinement phase, we calculate the baryon number density for the real baryon chemical potential  $\mu$  values via Eq. (8) with restricted number of terms to  $n_{max}$ .

The results are shown in Figs. 3 and 4. For large  $\mu/T$ , the number density obtained via Eq. (8) goes to plateau as a consequence of the finite number of terms in respective sums. The plateau is shifted to higher  $\mu/T$  with increasing the number of terms  $n_{max}$ .

We expect that increasing of statistics will allow us to increase  $n_{max}$ . The two results coincide within error bars up to  $\mu/T < 2.5$  at  $T/T_c = 1.35$  and  $\mu/T < 5.0$  at  $T/T_c = 0.93$ . In Figs. 3 and 4, we show also the analytic continuation results; They diverge as  $\mu/T$  increases and can not reach the plateau.

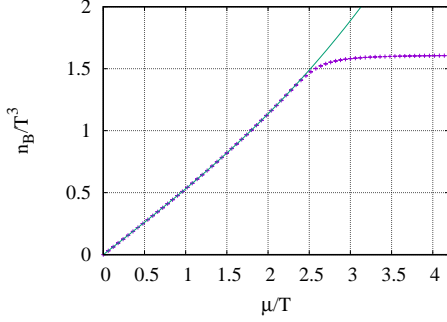


Figure 3: The baryon number density for the real chemical potential at  $T/T_c = 1.35$ . Green curve shows result of the analytic continuation.

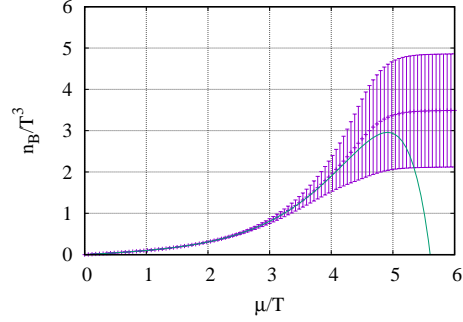


Figure 4: The baryon number density for the real chemical potential at  $T/T_c = 0.93$ . Green curve shows result of the analytic continuation.

### Pressure

In Figs. 5, and 6, we show dependence on the chemical potential of the pressure:  $\Delta P(\mu) = (P(\mu) - P(0)) / T^4$  at  $T = 1.35T_c$  and  $0.93T_c$  as a function of  $\mu/T$ .

For small  $\mu/T$ ,  $\Delta P$  behaves as quadratic function, while for high  $\mu/T$ , it has the linear form.

### Moments of the baryon number density

In the relativistic heavy-ion collision experiments,  $\lambda_2/\lambda_1$  and  $\lambda_4/\lambda_2$  (kurtosis) are expected to be good indicators for detecting the QCD phase transition [2, 17]. We calculate these quantities and compare with experiments. In Ref. [18], the canonical partition functions,  $Z_n$ , were extracted from the RHIC experiments data. One can construct  $\lambda_2/\lambda_1$  and  $\lambda_4/\lambda_2$  from these  $Z_n$ . In Figs. 7 and 8, we show these ratios as calculated by the integration method described above together with those extracted from the RHIC Star data at  $\sqrt{s_{NN}} = 62.4$  GeV.

We choose  $\sqrt{s_{NN}} = 62.4$  GeV because it corresponds to freeze-out temperature  $T = 149.9 \pm 0.5$  MeV (the closest to our  $T/T_c = 0.93$ ) and small

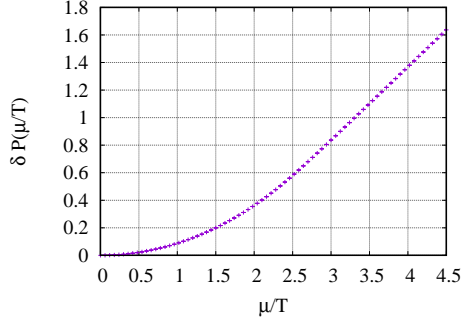


Figure 5: Pressure at  $T/T_c = 1.35$ .

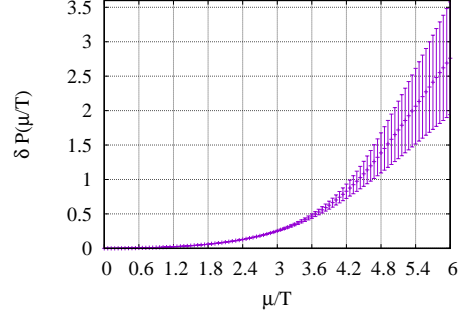


Figure 6: Pressure at  $T/T_c = 0.93$ .

chemical potential, as it is estimated in Refs. [19] and [20]. The ratios of  $\lambda_2/\lambda_1$  and  $\lambda_4/\lambda_2$  at  $T/T_c = 1.35$  are shown in Figs. 9 and 10.

Note that  $Z_n$  were constructed from the proton multiplicity data, not the baryon multiplicity. Therefore, the results should be considered as a proxy for the real baryon number moments. Nevertheless, in the confinement regions we see very good agreement for  $\lambda_2/\lambda_1$  and  $\lambda_4/\lambda_2$  between the lattice calculation and those estimated from RHIC data.

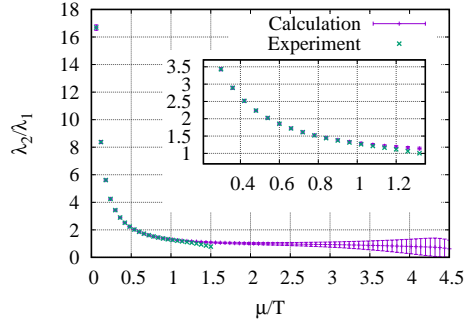


Figure 7: Ratio of the moments  $\lambda_2/\lambda_1$  at  $T/T_c = 0.93$ . The green line is  $\lambda_2/\lambda_1$  constructed from the RHIC STAR experimental data at  $\sqrt{s_{NN}}=62.4\text{GeV}$ .

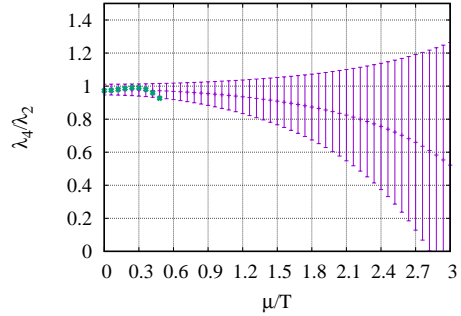


Figure 8: Ratio of the moments  $\lambda_4/\lambda_2$  at  $T/T_c = 0.93$ . The green line is  $\lambda_4/\lambda_2$  constructed from the RHIC star experimental data at  $\sqrt{s_{NN}}=62.4\text{GeV}$ .

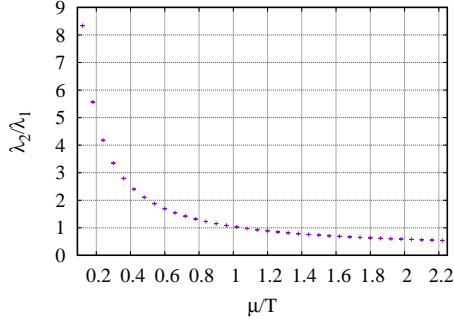


Figure 9: Ratio of the moments  $\lambda_2/\lambda_1$  at  $T/T_c = 1.35$

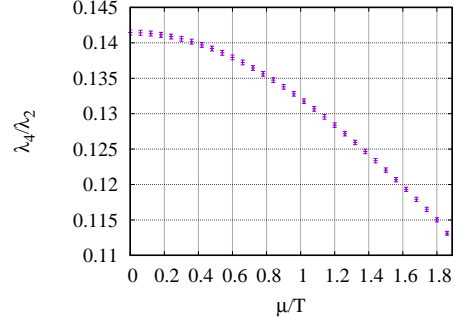


Figure 10: Ratio of the moments  $\lambda_4/\lambda_2$  at  $T/T_c = 1.35$ .

## 5. Concluding Remarks

In this letter, we study an approach for revealing the QCD phase structure using lattice QCD simulations. Prior to this study, it was believed that this was impossible because of the sign problem; only small density regions could be studied by extrapolating from the data at  $\mu = 0$ . However, all relevant information on the QCD phase at finite baryon density is contained in the imaginary chemical potential regions,  $0 \leq \mu_I/T \leq \pi$ . The question is how to map this information to the real chemical potential. Eq. (4) provides a possible solution, because  $Z_n$  can be calculated in the imaginary chemical potential regions. Since numerical Monte Carlo simulations provide results with finite accuracy, we should find practical methods which work.

We fit the number density at the imaginary chemical potential using  $Z_n$  as parameters and found that it does not work.

We parametrize the number density in the imaginary chemical potential with the Ansatz (the Fourier series in the confinement and polynomial series in the deconfinement) and integrate them to get the grand partition function.  $Z_n$  and other observables are then calculated from them.

This method produces  $Z_n$  up to  $n_{max}$  which is determined by used ansatz and current statistics. However, this is not the first principle calculation, because we introduce an assumption to the number density. Moreover, this misses the higher frequency contributions.

On the other hand, better interpolation procedure (cubic spline for example) or numerical integration rather than any Ansatz release our data from

assumptions. This study will be reported in future.

We studied how errors of calculations made at the imaginary chemical potential propagate into errors at the real one. We also found range of reliability of our results by imposing the condition that  $Z_n$  have to be positive.

We then investigate whether we can estimate  $\lambda_2/\lambda_1$  and  $\lambda_4/\lambda_2$ . The results are consistent with the values estimated from the RHIC experiments as shown in Figs. 7 and 8. This is very encouraging.

The lattice QCD simulation results presented here are exploratory: the quark mass is heavy and the lattice spacing is large. These problems can be overcome using modern lattice techniques and increasing computational power. Then, we can explore higher density regions and may detect the QCD phase transition by combining lattice calculations and experimental data.

## Acknowledgment

This work was completed thanks to support from RSF grant 15-12-20008. Work done by A. Nakamura on the theoretical formulation of  $Z_n$  for comparison with experiments was supported by JSPS KAKENHI Grant Numbers 26610072 and 15H03663. The calculations were performed on Vostok-1 at FEFU.

## References

- [1] L. Adamczyk, J. K. Adkins, G. Agakishiev, M. M. Aggarwal, Z. Ahammed, I. Alekseev, et al., Energy dependence of moments of net-proton multiplicity distributions at RHIC, *Physical Review Letters* 112 (2014) 032302. doi:10.1103/PhysRevLett.112.032302.
- [2] X. Luo, Probing the qcd critical point by higher moments of net-proton multiplicity distributions at STAR, *Open Physics* 10 (6) (2012) 1372–1374.
- [3] D. Kharzeev, M. Nardi, Hadron production in nuclear collisions at RHIC and high-density QCD, *Physics Letters B* 507 (1) (2001) 121–128.
- [4] T. Yokota, T. Kunihiro, K. Morita, Functional renormalization group analysis of the soft mode at the QCD critical point, *Progress of Theoretical and Experimental Physics* 2016 (7) (2016) 073D01.

- [5] H.-T. Ding, F. Karsch, S. Mukherjee, Thermodynamics of strong-interaction matter from lattice QCD, International Journal of Modern Physics E 24 (2015) 1530007. [arXiv:1504.05274](#), [doi:10.1142/S0218301315300076](#).
- [6] A. Bazavov, H.-T. Ding, P. Hegde, O. Kaczmarek, F. Karsch, E. Laermann, Y. Maezawa, S. Mukherjee, H. Ohno, P. Petreczky, H. Sandmeyer, P. Steinbrecher, C. Schmidt, S. Sharma, W. Soeldner, M. Wagner, QCD equation of state to  $\mathcal{O}(\mu_B^6)$  from lattice QCD, Physical Review D 95 (2017) 054504. [doi:10.1103/PhysRevD.95.054504](#).
- [7] J. Gunther, R. Bellwied, S. Borsanyi, Z. Fodor, S. Katz, A. Pasztor, C. Ratti, The QCD equation of state at finite density from analytical continuation (2016). [arXiv:1607.02493](#).
- [8] M. D’Elia, G. Gagliardi, F. Sanfilippo, Higher order quark number fluctuations via imaginary chemical potentials in  $N_f = 2 + 1$  QCD (2016). [arXiv:1611.08285](#).
- [9] S. Datta, R. V. Gavai, S. Gupta, Quark number susceptibilities and equation of state at finite chemical potential in staggered QCD with  $N_t = 8$  (2016). [arXiv:1612.06673](#).
- [10] A. Hasenfratz, D. Toussaint, Canonical ensembles and nonzero density quantum chromodynamics, Nuclear Physics B 371 (1) (1992) 539–549.
- [11] S. Ejiri, Y. Maezawa, N. Ukita, S. Aoki, T. Hatsuda, N. Ishii, K. Kanaya, T. Umeda, Equation of state and heavy-quark free energy at finite temperature and density in two flavor lattice QCD with Wilson quark action, Physical Review D 82 (2010) 014508. [arXiv:0909.2121](#), [doi:10.1103/PhysRevD.82.014508](#).
- [12] V. Bornyakov, D. Boyda, V. Goy, A. Molochkov, A. Nakamura, A. Nikolaev, V. Zakharov, New approach to canonical partition functions computation in  $N_f = 2$  lattice QCD at finite baryon density (2016). [arXiv:1611.04229](#).
- [13] D. L. Boyda, V. G. Bornyakov, V. A. Goy, V. I. Zakharov, A. V. Molochkov, A. Nakamura, A. A. Nikolaev, Novel approach to deriving the canonical generating functional in lattice QCD at a fi-

- nite chemical potential, JETP Letters 104 (10) (2016) 657–661. doi:10.1134/S0021364016220069.
- [14] M. D’Elia, F. Sanfilippo, Thermodynamics of two flavor QCD from imaginary chemical potentials, Physical Review D 80 (1) (2009) 014502. arXiv:0904.1400, doi:10.1103/PhysRevD.80.014502.
  - [15] T. Takaishi, P. de Forcrand, A. Nakamura, Equation of state at finite density from imaginary chemical potential, in: PoS LATTICE 2009, 2010. arXiv:1002.0890.
  - [16] J. Takahashi, H. Kouno, M. Yahiro, Quark number densities at imaginary chemical potential in  $N_f = 2$  lattice QCD with Wilson fermions and its model analyses, Physical Review D 91 (1) (2015) 014501.
  - [17] K. Redlich, Probing the QCD chiral cross-over transition in heavy ion collisions, Central European Journal of Physics 10 (6) (2012) 1254–1257. doi:10.2478/s11534-012-0105-0.
  - [18] A. Nakamura, K. Nagata, Probing QCD phase structure using baryon multiplicity distribution, Progress of Theoretical and Experimental Physics 2016 (3) (2016) 033D01.
  - [19] J. Cleymans, H. Oeschler, K. Redlich, S. Wheaton, Comparison of chemical freeze-out criteria in heavy-ion collisions, Physical Review C 73 (3) (2006) 034905.
  - [20] P. Alba, W. Alberico, R. Bellwied, M. Bluhm, V. Mantovani Sarti, M. Nahrgang, C. Ratti, Freeze-out conditions from net-proton and net-charge fluctuations at RHIC, Physical Review B 738 (2014) 305–310. arXiv:1403.4903, doi:10.1016/j.physletb.2014.09.052.